

# Efficient Effective Permittivity Treatment for the 2D-FDTD Simulation of Photonic Crystals

T. Jalali<sup>1,4,5,\*</sup>, K. Rauscher<sup>1,6</sup>, A. Mohammadi<sup>5</sup>, D. Erni<sup>1,3</sup>, Ch. Hafner<sup>2</sup>,  
W. Baechtold<sup>1</sup>, and M. Z. Shoushtari<sup>4</sup>

<sup>1</sup>Communication Photonics Group, <sup>2</sup>Computational Optics Group,  
Laboratory for Electromagnetic Fields and Microwave Electronics,  
ETH Zurich, 8092 Zurich, Switzerland

<sup>3</sup>General and Theoretical Electrical Engineering (ATE), Faculty of Engineering,  
University of Duisburg-Essen, 47048 Duisburg, Germany

<sup>4</sup>Physics Department, Shahid Chamran University, Ahvaz, Iran

<sup>5</sup>Physics Department, Persian Gulf University, Bushehr, Iran

<sup>6</sup>Eurospace GmbH, 60313 Frankfurt, Germany

In this paper, we present an efficient effective permittivity treatment for the two-dimensional Finite-Difference Time-Domain (2D-FDTD) method that can be applied to dielectric interfaces. Various issues related to simulation arrangements are discussed based on the 60° photonic crystal (PhC) waveguide bend as a test case. The transmission, obtained numerically, agrees very well with other two-dimensional simulation methods, namely the finite-element method (2D-FEM) and the 2D multiple multipole program (2D-MMP). Compared to other FDTD schemes, such as staircasing and the volume averaging method, our model performs faster and provides more accurate results for the dielectric interface.

**Keywords:** Photonic Crystal, Photonic Crystal Waveguide, FDTD Method.

## 1. INTRODUCTION

Research in advanced optics, especially in the area of nanoscale science, leads to ultra-compact multi-functional photonic integrated devices. The control of the light field in such devices demands an increased complexity of the underlying structure. To face the large diversity provided by the various device shapes, computational optics methods based on volume-discretization have proven most practical. A straightforward implementation is the FDTD approach. It has several advantages, such as simplicity of the underlying update algorithm. Furthermore, large index contrasts can easily be handled. However, in FDTD simulation the accurate treatment of the material interface is an important issue to be further investigated. In the FDTD scheme the discretization of the model is usually done by a Cartesian grid. This grid, applied to arbitrarily curved shapes, leads to rectangular cells partially filled with different dielectric permittivities. These cells are often substituted with an effective permittivity to account for the offsets on this dielectric interfaces. However, this analysis

should be done carefully due to the discontinuity of the fields or its derivatives at dielectric interfaces. Different kinds of effective permittivity methods had been proposed: volume averaging, mixing formula like, Maxwell-Garnett, and Bruggeman formula.<sup>1</sup> Here, we propose a new treatment for an effective permittivity in the Yee algorithm that is more efficient and accurate with respect to other kind of effective permittivity methods. As a suitable test case we have analyzed a PhC waveguide bend.<sup>2</sup> The periodic structure of a PhC results in a large amount of interface regions with respect to the analyzed volume. Moreover, the staircasing effect becomes increasingly important especially for shapes with small feature sizes. In order to provide a large photonic band gap, the underlying PhC structure should have a large refractive index contrast as well as a large air filling factor. Both issues challenge any kind of accurate interface treatment and are therefore well suited to validate our numerical approach for the effective permittivities.

In the reminder of the paper, we will propose an efficient model based on effective permittivities to deal with the proper domain discretization at dielectric interfaces for the 2D-FDTD methods. The 2D-FDTD implementation

\* Author to whom correspondence should be addressed.

is validated using a 60° PhC waveguide bend and also the upgraded 2D-FDTD code with conventional FDTD discretization schemes is compared. Furthermore, we qualify our model against other methods such as the 2D-FEM and 2D-MMP.

## 2. EFFICIENT SCHEMES FOR EFFECTIVE PERMITTIVITY

The FDTD technique is a direct implementation of Maxwell’s time-dependent curl equations.<sup>3</sup> It solves the temporal variation of electromagnetic waves within a finite space that contains an object of arbitrary geometry that is defined by assigned electromagnetic constants including permittivity and permeability over the grid points. Without loss of generality and referring to the specific PhC realization, we have considered only the transverse electric (TE) polarization. By using a broadband Gaussian pulse excitation with a temporal envelope  $e^{-(t-t_0)^2/2\sigma^2}$  around a light carrier with  $\omega_0$ , the frequency response of the PhC device can be obtained in only one FDTD run. Here,  $\sigma$  reflects the pulse width in order to cover the bandwidth of the device’s power transmission and  $t_0$  is the time delay. Due to the finite size of the computational domain, CPMLs are used as the absorbing boundaries. Their implementation is based on the time-dependent form of the stretched coordinate formulation and a recursive convolution. Compared to other absorbing boundary conditions, CPMLs are highly absorptive for evanescent waves, require significantly less computational memory and provide a straightforward implementation. To obtain the frequency response, the values have to be converted to the frequency domain, for which a discrete Fourier transform (DFT) is used. For analyzing the performance of a guiding structure, the time-averaged power flow is monitored.

Arbitrarily shaped dielectric surfaces, such as e.g., a periodic array of holes in a PhC, generate partially filled FDTD cells. In the staircasing method, these cells are approximated by either an empty cell or completely filled cells. Therefore, the numerical cells representation is different from the real one and causing errors in the computation. A more efficient approach than choose a finer mesh is to assign an effective permittivity for these partially field cells. In 2D, this problem is subdivided with respect to the TE and TM mode. In the TM case, the electric field polarization is always parallel to the interface, so equation (1) is accurate enough to calculate the effective permittivity.<sup>4-7</sup> The electric field in the considered TE case impinges with different angles at the interface between the two media. In our approach, we assume an electric field that is either parallel or perpendicular to the interfaces (Fig. 1) and we neglect those configurations of the cells, where less than half of the cell is filled. The calculation of the effective permittivity requires both the tangential and the normal components of the electric field: If the electric

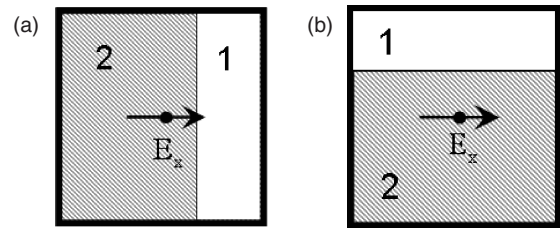


Fig. 1. Partially filled cells: (a) interface orthogonal to the electric field component and (b) interface parallel to the electric field component.

field is parallel to the interface, the effective permittivity can be derived from the integral form of Ampere’s law. If the electric field is perpendicular to the interface, it follows from the integral form of the Faraday law. Both parallel and perpendicular contributions to the effective permittivity are readily computed as:<sup>1</sup>

$$\epsilon_{\parallel} = f\epsilon_2 + (1 - f)\epsilon_1 \tag{1}$$

$$\epsilon_{\perp} = \left( \frac{f}{\epsilon_2} + \frac{(1-f)}{\epsilon_1} \right)^{-1} \tag{2}$$

Where  $f$  is the ratio of the filled area of the cell to the cell’s area and  $\epsilon_1, \epsilon_2$  are the dielectric permittivity of media 1 and 2, respectively. For curved surfaces, the effective permittivity is the superposition of the normal and the parallel effective permittivity with respect to the angle between electric field and boundary. We utilize the phenomenological relation that has been carried out in an earlier publication<sup>1</sup>

$$\epsilon_{\text{eff}} = \epsilon_{\parallel} \cos^2 \theta + \epsilon_{\perp} (1 - \cos^2 \theta) \tag{3}$$

Where  $\theta \in [0, \pi/2]$  encompasses the angle between the electric field vector and the normal vector to the boundary. The Eq. (3) reduces to Eqs. (1) and (2) for  $\theta = 0$  and  $\pi/2$ , respectively. We calculate the average of the angle  $\theta$  between the electric field and the boundary outgoing from the center of radius of curvature for each cell. Our approach is therefore called projected effective permittivity (PEP) treatment. It makes the calculation of effective permittivity more accurate compared to the other publications.<sup>1,4-7</sup> It follows for partially filled cells (Fig. 2) that different PEP should be considered for the  $x$  and  $y$  components of the electric field. PEP allows a straightforward implementation into the Yee algorithm. Instead of using regular permittivity, one uses PEP for  $E_x$  and  $E_y$  separately, i.e., for each time step in the Maxwell equations for the TE mode, we have to calculate  $\epsilon_{\text{eff},x}$  and  $\epsilon_{\text{eff},y}$ . As shown in the following, PEP is more accurate than the other averaging methods. The main reason for this is that it contains more information about the boundary, and, hence, we have a more accurate partial cell representation in the context of different effective permittivities. Since PEP is calculated during pre-processing the algorithm remains as fast and memory efficient as the basic

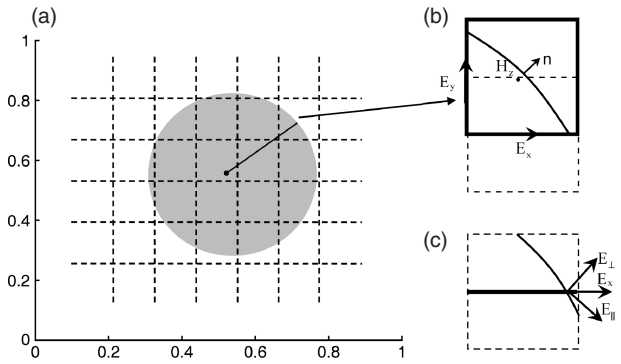


**Fig. 2.** (a) FDTD mesh for a curved surface, dashed: grid line. (b) field components for H-modes in one partially filled cell, dashed: Ampere contour path for integration, (c)  $x$  component of the electric field and normal and tangential projection relative to the interface.

Yee algorithm. It just needs a bit more memory to store the effective permittivity values. PEP is particularly important when the index contrast is high.

### 3. THE 60° PHOTONIC CRYSTAL WAVEGUIDE BEND

Photonic crystal (PhC) devices were well studied in recent years since they possess as unique features as a photonic band gap in which light is not permitted to propagate. While introducing line defects into the PhC, however, light of certain wavelengths is mainly allowed to propagate along the defect lines, which gives rise to a light guiding mechanism. The vertical light confinement is provided by total internal reflection when layered semiconductor slabs are considered as the PhC's underlying material system. In the 2D simulations, the PhC's background material is associated to an effective index which refers to the corresponding planar PhC structure, where the vertical layer stack is characterized to the following parameters: Indium Phosphid/Indium Gallium Arsenide Phosphid (InP/InGaAsP) low refractive index material system, with an effective index of  $n = 3.24$  (layer stack: InP [200 nm]/InGaAsP [434 nm]/InP [600 nm]/InP substrate) and a  $r/a$  of 0.33 (hole radius divided by lattice constant), corresponding to a filling factor of 35%, providing a wide photonic band gap (PBG) around an operating wavelength of  $1.55 \mu\text{m}$  (Ref. [2]). In a PhC, light bending within a length scale comparable to the wavelength is achievable. The bent waveguide selected as test case here, follows the hexagonal lattice symmetry and, hence, the bending angle is  $60^\circ$ . The whole bend is very compact and covers an area of  $5 \times 4$  lattice constants. The spectral response of the non-optimized bend is depicted in Figure 3(a) yielding a narrow power transmission band ( $\sim 10\%$  of the overall PBG) near the low-frequency photonic band edge. Using structural optimization, we achieve an improvement of this bandwidth by shifting certain holes in the immediate bending region of the PhC bend. These holes are specified by a

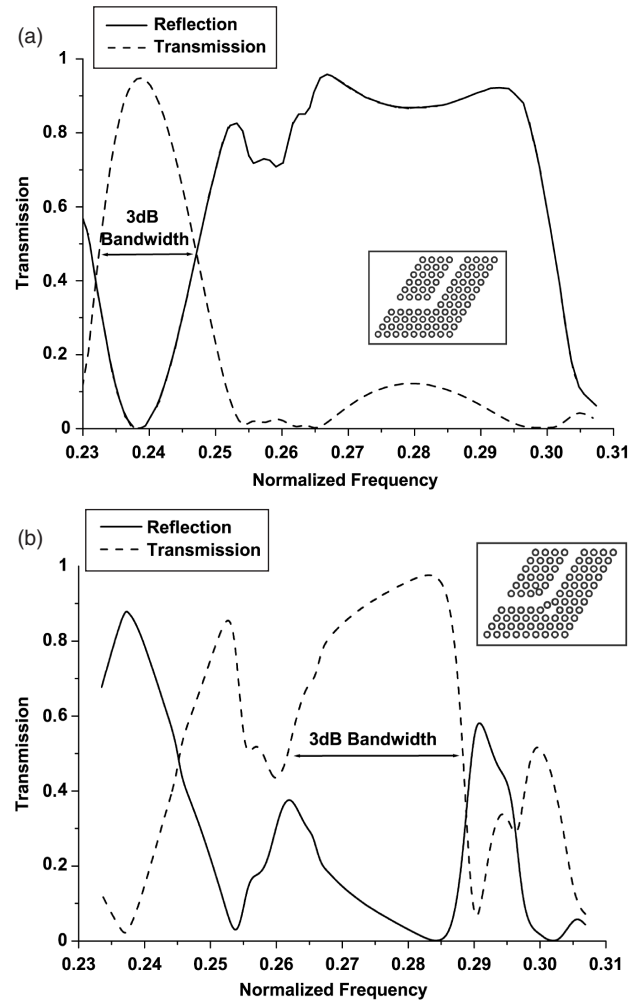


**Fig. 3.** (a) Power transmission and reflection of a non-optimized  $60^\circ$  PhC bend. (b) The optimized bend with properly reshaped bending region.

sensitivity analysis. The underlying optimization has been published elsewhere.<sup>2</sup> The resulting performance yields a bandwidth of 29% of the whole PBG and a maximum power transmission of 96.8% (Fig. 3(b)).

When a structure is optimized by fine-tuning geometric parameters such as the radii and the locations of holes in the PhC structures, some areas of the structures may become very sensitive with respect to the spectral characteristics of the entire structure.<sup>2</sup> In the test case, this is the area near the bend, where some sort of cavity was generated by the optimization process. The simulation of such optimized structures is usually much more demanding the simulation of the original, more primitive ones. Therefore, optimized structures pose hard test cases for new methods.

### 4. COMPARISON AND DISCUSSION

We have validated our PEP-2D-FDTD method against the most commonly used effective permittivity models in 2D-FDTD such as volume-averaging and staircasing. As a

further validation step, the optimized PhC waveguide bend structure is used to compare the proposed PEP-2D-FDTD with two commercially available frequency-domain simulators, namely FEMLAB<sup>8</sup> based on the finite elements (FE) method, and the Multiple Multipole Program (MMP) contained in the MaX-1 software package,<sup>9</sup> which is based on a semi-analytical extension of the Mie-Vekua theory. The 2D-FDTD environment is discretized by a square grid with the side length of 67 nm and uses a convolutional PML (CPML) for the termination of the computational window. In PhC waveguide simulations highly absorbing boundary conditions are needed in order to minimize the large reflections stemming from the mismatch at the proper PhC waveguide input and output, respectively.<sup>10</sup> Therefore, a thick CPML with 24 layers has been introduced to minimize the error due to the unphysical reflection from the PhC waveguide terminations. The simulation region is  $300 \times 150$  cells in the computational space. To ensure the stability of the algorithm, the time step is chosen  $0.95/c\sqrt{x^{-2} + y^{-2}}$ , where  $c$  is the speed of light.<sup>3</sup> The numbers of CPML layers is 24, the order of spatial variation of the conductivity profile inside the layer is 1, and the conductivity at the end of the CPML layer is set to 0.2. The waveguide source is located in the middle of the waveguide input. The lowest order TE mode is generated for a slab waveguide. The width of the slab matches the size of the W1 waveguide, i.e., a one row of holes is omitted in order to obtain the waveguide. The number of sampling points for carrying out the DFT is set to 500. The simulation is done with 40000 time steps. In Figure 4(a) the staircasing and volume-averaging effective permittivity methods are compared with PEP-FDTD, where staircasing and the volume-averaging show oppositely shifted power transmission spectra, with a blueshift of  $+0.065$  (in normalized frequency) for the staircasing and a redshift of  $-0.10$  for the volume-averaging method. This effects are attributed to the variations in the residual hole volumes that emerges from the two different discretization methods applied to the hole shape. The PEP-2D-FDTD is also compared to the 2D-FE and 2D-MMP, where the latter will act as an accurate reference due to its semi-analytical nature. In the FDTD and FEM simulation spectra additional peaks in the normalized frequency region from 0.255 to 0.266 are visible. They are due to the superposition of modes transmitted or reflected on the bend and the PhC waveguide interfaces. This contrasts the MMP simulations because its underlying methodology allows the implementation of perfect excitation and matching conditions at the accessing waveguide ports, leading to highly reliable spectral responses of both, the PhC bend's power transmission and power reflection.<sup>11</sup> The results of all calculations match very well in terms of transmission quantity and bandwidth behavior. The coincidence of the spectra confirms the superiority of the PEP-2D-FDTD against other permittivity models (Fig. 4(a)) and renders the PEP scheme to be

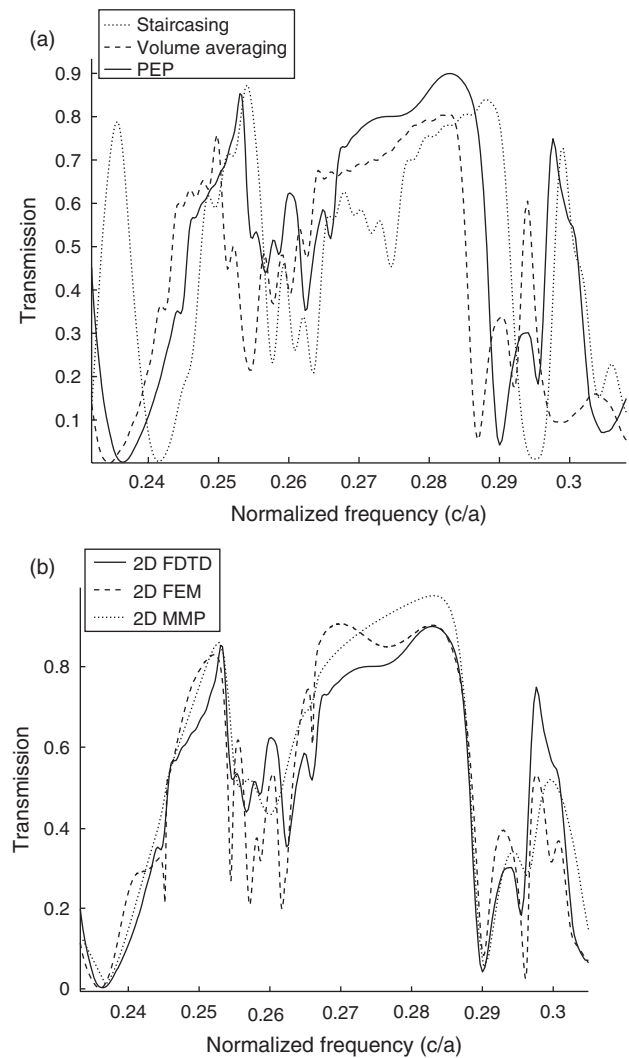


**Fig. 4.** Optimized bend: (a) Comparison of different permittivity models for 2D-FDTD. (b) Comparison of different simulation methods.

competitive to even more adapted discretization schemes used, e.g., in FE and MMP. Uusitupa reported a shift of the transmission spectra in frequency after using a coarse grid with large cell sizes.<sup>12</sup> The good match between PEP-FDTD and the other simulation methods infers that PEP will be still accurate even by using bigger cell sizes, leading to shorter simulation times. PEP method improves the accuracy of FDTD method and therefore allows one to use coarser meshes while lowering the computation time.

## 5. CONCLUSION

We have developed a simple method for modeling electromagnetic wave propagation in arbitrarily shaped dielectric media by using a modified FDTD scheme. We have improved the Cartesian FDTD scheme by evaluating the dielectric constant for partially empty cells based on PEP with respect to their angles. We also increased the efficiency of the FDTD program by employing the CPML

technique. The accuracy of our approach was investigated by comparing this improved FDTD scheme with other simulation methods. PEP-FDTD only needs more sophisticated pre-processing but this does not significantly affect the total computation time that is certainly dominated by the FDTD updating effort.

Numerical results have shown that the impact of discretization at a discontinuity between two media can be reduced. Comparisons have been made for a 60° PhC waveguide bend. The staircasing and volume-averaging method showed substantial differences in the transmission spectra. However, the PEP-FDTD method has a good agreement with results computed with FEM and 2D-MMP codes. It's worth mentioning that the straightforward and easy to realize methodology behind PEP has led to a 2D-FDTD code where the impact of discretization at a discontinuity between two media is significantly reduced and which is both, faster and more accurate than standard FDTD implementations.

## References

1. A. Mohammadi, H. Nadgaran, and M. Agio, *Opt. Express*. 13, 10367 (2005).
2. K. Rauscher, D. Erni, J. Smajic, and C. Hafner, *Prog. Elec. Research Sym. PIERS 2004* 43, 25 (2004).
3. A. Taflove, *Computational Electrodynamics, the Finite-Difference Time-Domain Method*, Norwood, Artech House, MA (2005).
4. J. G. Maloney and G. S. Smith, *IEEE Trans. Antennas Propag.* 40, 323 (1992).
5. N. Kaneda, B. Houshmand, and T. Itoh, *IEEE Trans. Microwave Theory Tech.* 45, 1645 (1997).
6. T. Hirono, Y. Shibata, W. W. Lui, S. Seki, and Y. Yoshikuni, *IEEE Microwave Guided Wave Lett.* 10, 359 (2000).
7. K. P. Hwang and A. C. Cangellaris, *IEEE Microwave Wireless Comp. Lett.* 11, 158 (2001).
8. <http://www.comsol.com>
9. <http://www.MAX-1.ethz.ch>
10. A. Mekis, S. Fan, and J. D. Joannopoulos, *IEEE Microwave Guided Wave Lett.* 9, 502 (1999).
11. E. Moreno D. Erni, and C. Hafner, *Phys. Rev. E* 66, 3 (2002).
12. T. Uusitupa, K. Kaerkaeinen, and K. Nikoskinen, *Microwave Opt. Technol. Lett.* 39, 326 (2003).

Received: 31 October 2006. Accepted: 8 November 2006.